

Nuclear parton distributions at next to leading order

D. de Florian* and R. Sassot†

*Departamento de Física, Facultad de Ciencias Exactas y Naturales, Universidad de Buenos Aires,
Pabellón I, Ciudad Universitaria (1428) Buenos Aires, Argentina*

(Received 19 November 2003; published 28 April 2004)

We perform a next to leading order QCD global analysis of nuclear deep inelastic scattering and Drell-Yan data using the convolution approach to parametrize nuclear parton densities. We find both a significant improvement in the agreement with data compared to previous extractions, and substantial differences in the scale dependence of nuclear effects compared to leading order analyses.

DOI: 10.1103/PhysRevD.69.074028

PACS number(s): 13.60.Hb, 12.38.Bx, 24.85.+p

I. INTRODUCTION

Ever since the discovery, two decades ago, that quark and gluons in bound nucleons show momentum distributions noticeably different from those measured in free or less bound nucleons [1], the precise determination of nuclear parton densities has awakened growing attention, driving both increasingly precise and comprehensive nuclear structure function measurements [2], and a more refined theoretical understanding of the underlying physics. The precise knowledge of nuclear parton distribution functions (NPDFs) is not only required for a deeper understanding of the mechanisms associated with nuclear binding from a QCD improved parton model perspective, but it is also the starting point for the analyses of a wide variety of future and ongoing high energy physics experiments, such as heavy ion collisions at Relativistic Heavy Ion Collider (RHIC) [3], proton-nucleus collisions to be performed at CERN Large Hadron Collider (LHC) [4], or neutrino-nucleus interactions in long baseline neutrino experiments [5], for example. Consequently, the accuracy of NPDF is rapidly evolving into a key issue in many areas of particle physics.

From the point of view of perturbative QCD, the extraction of NPDFs can be done in close analogy with what is done for free nucleons: they are considered as nonperturbative inputs, to be inferred from data, whose relation to the measured observables and energy scale dependence are computed order by order in perturbation theory. Although one cannot discard larger higher twist power corrections than in the case of free nucleons, or even some sort of nuclear recombination effect, factorization and universality of NPDFs are expected to hold in a very good approximation, over a wide kinematical range in the present experiments.

At variance with nucleon PDFs, which driven by the demand of more and more precise predictions, have attained in the last years an impressive degree of accuracy and refinement, NPDF extractions are in a considerably earlier stage of the development. Not only is the number and diversity of nuclear data much more reduced, but the analyses are restricted to leading order (LO) accuracy, with rather crude parametrizations of nuclear effects which lead to poor

χ^2/N_{DF} values in global QCD fits to data [6,7].

There are also some caveats inherent to the particular approaches implemented so far, that define NPDF in terms of nucleon PDFs and a multiplicative nuclear correction factor at a given initial energy scale, from where they are evolved. In the first place, NPDFs defined in this way have their momentum fraction per nucleon restricted to be less than or equal to unity, what excludes from the description, and also from the evolution, a portion of its natural kinematical range. Of course, unless one is specifically interested in that region, this approximation is expected to imply a minor correction, although one cannot discard the excluded region as a source of new and interesting information.

Much more problematic in these approaches is that the actual shape of the nuclear correction factor required to reproduce accurately the data implies very capricious functions, with a large number of parameters, and which in practice precludes the numerical computation of the scale dependence at next to leading order (NLO) accuracy. The actual computation of structure functions and evolution equations at this order implies several convolution integrals very difficult to evaluate unless Mellin transform techniques are applied.

In this paper we show that a much more convenient alternative to deal with nuclear effects is to define NPDFs using a convolution approach. In such a framework the free nucleon parton densities are convoluted with very simple weight functions that parametrize nuclear effects. The convolution method naturally takes into account the actual range of nucleon momentum fractions, allows via Mellin transform techniques a straightforward numerical evaluation of the NLO scale dependence, leads to extraordinarily accurate NPDFs with relatively few parameters, and, finally, allows us to interpret the nuclear modifications in terms of a very simple mechanism of rebalance of momentum fractions between the distributions. The success of the convolution approach comes from the fact that the momentum fraction dependence of nuclear effects is strongly correlated to that of partons in free nucleons, as shown in rescaling models [8], a feature which is explicitly included by the convolution.

As an example of feasibility of the convolution approach we obtain for the first time a full NLO extraction of NPDFs from a large number of nuclear DIS [9–12] and Drell-Yan data [13]. We also assess the differences between the LO and NLO extractions, finding that although the quality of fits to

*Electronic address: deflo@df.uba.ar

†Electronic address: sassot@df.uba.ar

present data is comparable in both approximations, there are important differences between the Q^2 dependence of the nuclear correction factors using either LO or NLO extractions. This, for example, questions the use of LO factors with NLO nucleon parton densities to generate NPDFs in NLO computations, as it is common practice.

In the following section we summarize the main motivation and features of the convolution approach. In the third section we present the details and outcome of the NLO and LO NPDF extractions, comparing our results with previous LO analyses. In the last section we discuss the differences between LO and NLO extractions of NPDFs, computing the one hadron production cross section with them as an example, and present our conclusions.

II. NPDF

The description of DIS processes off nuclear targets $eA \rightarrow e'X$ is customarily done in terms of the hard scale Q^2 , defined as minus the virtuality of the exchanged photon and a scaling variable x_A , and the analogue to the Bjorken variable used in DIS off nucleons

$$Q^2 \equiv -q^2, \quad x_A \equiv \frac{Q^2}{2p_A \cdot q}, \quad (1)$$

respectively. Here p_A is the target nucleus momentum and consequently, x_A is kinematically restricted to $0 < x_A < 1$, just as with the standard Bjorken variable. Alternatively, one can define another scaling variable $x_N \equiv Ax_A$, where A is the mass number of the nucleus. Under the assumption that the nucleus momentum p_A is evenly distributed between that of the constituent nucleons $p_N = p_A/A$, this variable resembles the Bjorken variable corresponding to the scattering off free nucleons $x_N \equiv Q^2/(2p_N \cdot q)$. However, in a nuclear scattering context, of course, it spans the interval $0 < x_N < A$, by definition, and reflects the fact that a parton may in principle carry more than the average nucleon momentum.

When discussing NPDFs the usual approach is to propose a very simple relation between the parton distribution of a *proton* bound in the nucleus f_i^A and those for free protons f_i

$$f_i^A(x_N, Q_0^2) = R_i(x_N, Q_0^2, A, Z) f_i(x_N, Q_0^2) \quad (2)$$

in terms of a multiplicative nuclear correction factor $R_i(x_N, Q^2, A, Z)$, specific for a given nucleus (A, Z) , parton flavor i , and initial energy scale Q_0^2 . This description is convenient since the ratio $R_i(x_N, Q^2, A, Z)$ directly compares the parton densities with and without nuclear effects, and is closely related to the most usual nuclear DIS observables, which are the ratios between the nuclear and deuterium structure functions. Indeed, we will use this picture to simplify the presentation of the output of our analysis. However, this is not the best suited way to parametrize the effects in the intermediate steps of the analysis, nor the best alternative for higher order numerical computations, as was mentioned previously.

Since $f_i(x_N, Q_0^2)$ are defined for $0 < x_N < 1$, NPDFs defined as in Eq. (2) are *a priori* restricted to that same range at

the initial scale. In most analyses the evolution equations are also constrained to $0 < x_N < 1$, losing the possibility of analyzing nuclear effects beyond $x_N > 1$ at any other scale. Notice that even if NPDFs were constrained to be zero for $x_N > 1$ at a given scale, the complete evolution equations would produce nonzero values for other scales in the range of x_N neglected by the approach, leading to a possible violation of momentum conservation. On the other hand, the direct parametrization of the ratios $R_i(x_N, Q^2, A, Z)$ require many parameters and even x_N dependencies whose Mellin moments cannot be put into a closed expression.

A much more adequate alternative to Eq. (2) is to relate NPDFs to standard PDFs by means of a convolution

$$f_i^A(x_N, Q_0^2) = \int_{x_N}^A \frac{dy}{y} W_i(y, A, Z) f_i\left(\frac{x_N}{y}, Q_0^2\right), \quad (3)$$

where the weight function $W_i(y, A, Z)$ now parametrizes the nuclear effects and can be thought of as the effective density of nucleons within the nucleus carrying a fraction y/A of its longitudinal momentum. In addition to allowing the full kinematical range for NPDFs, this kind of approach has been shown to lead to remarkably good parametrizations of nuclear effects with very few parameters, and with a smooth A dependence [14]. For example, neglecting nuclear effects, the effective nucleon density is just $W_i(y, A, Z) = A \delta(1 - y)$, and simple shifts in the momentum fraction carried by nucleons $W_i(y, A, Z) = A \delta(1 - y - \epsilon)$ have been shown to reproduce in a very good approximation many features of the known nuclear modifications to structure functions.

The convolution approach also allows us to perform the evolution in Mellin space, which is much more convenient numerically, and almost mandatory for NLO accuracy. Defining $y_A \equiv y/A$, Eq. (3) reads

$$f_i^A(Ax_A, Q_0^2) = \int_{x_A}^1 \frac{dy_A}{y_A} W_i(y_A, A, Z) f_i\left(\frac{x_A}{y_A}, Q_0^2\right) \quad (4)$$

and in Mellin space, i.e., taking moments in both sides of Eq. (4),

$$\hat{f}_i^A(N, Q_0^2) = \hat{W}_i(N, A, Z) \hat{f}_i(N, Q_0^2), \quad (5)$$

where

$$\hat{f}_i^A(N, Q_0^2) \equiv \int_0^1 dx x^{N-1} f_i^A(Ax, Q_0^2) \quad (6)$$

and similarly for $\hat{f}_i(N, Q_0^2)$ with $A = 1$, and

$$\hat{W}_i(N, A, Z) \equiv \int_0^1 dx x^{N-1} W_i(Ax, A, Z). \quad (7)$$

Notice that the moments are defined in terms of the correct scaling variable x_A , and that the evolution of the NPDF moments $\hat{f}_i^A(N, Q_0^2)$ can be managed with a standard evolution code in Mellin space.

Nuclear structure functions are defined as the average of the proper combination of the bound proton and neutron structure functions as

$$AF_2^A(x, Q^2) = ZF_2^{p/A}(x, Q^2) + (A-Z)F_2^{n/A}(x, Q^2), \quad (8)$$

where both bound nucleon structure functions can be written in terms of the corresponding nuclear parton distributions in Mellin space as

$$F_2^{p/A}(N-1, Q^2) = \sum_{q,q} e_q^2 \left\{ \hat{f}_i^A(N, Q^2) + \frac{\alpha_s}{2\pi} [C_q^{(1)}(N) \times \hat{f}_i^A(N, Q^2) + C_g^{(1)}(N) \hat{f}_g^A(N, Q^2)] \right\}. \quad (9)$$

The first term on the right hand side of Eq. (9) corresponds to the leading-order contribution while the second represents the next-to-leading order correction. Expressions for the NLO quark and gluon coefficients $C_q^{(1)}(N)$ and $C_g^{(1)}(N)$ can be found in Ref. [15]. In our analysis we consider only 3 active flavors and neglect the contribution from heavy quarks to the structure function.

Considering that DIS data do not allow us to determine all combinations of flavors, and that nuclear effects may be expected to be isospin invariant in a first approximation, it seems to be reasonable to introduce only three independent $\hat{W}_i(y, A, Z)$: one for the valence distributions, another for the light sea, and the last for the gluons. In this way

$$\begin{aligned} u_v^A(N, Q_0^2) &= \hat{W}_v(N, A, Z) u_v(N, Q_0^2), \\ d_v^A(N, Q_0^2) &= \hat{W}_v(N, A, Z) d_v(N, Q_0^2), \\ \bar{u}^A(N, Q_0^2) &= \hat{W}_s(N, A, Z) \bar{u}(N, Q_0^2), \\ \bar{d}^A(N, Q_0^2) &= \hat{W}_s(N, A, Z) \bar{d}(N, Q_0^2), \\ g^A(N, Q_0^2) &= \hat{W}_g(N, A, Z) g(N, Q_0^2). \end{aligned} \quad (10)$$

Notice that in many proton parton densities, and in particular in GRV98 [16], the one will be used in the following, the strange and heavy quark densities vanish at the low initial scale and there is no need to introduce additional weight functions for the latter. The parton distributions for the bound neutron can be obtained from the ones above by isospin symmetry.

An interesting feature in this approach is that since non-singlet combinations of parton densities, as those for valence quarks, evolve independently, and both $\hat{f}_i^A(N, Q^2)$ and $\hat{f}_i(N, Q^2)$ obey the same evolution equations, the moments of the weight function $\hat{W}_i(N, A, Z)$ are scale independent [17]. This is not the case for sea or gluon weight functions, since they are affected by singlet evolution resulting in a scale dependence due to quark and gluon mixing and therefore needed to be defined at a particular scale.

Charge, baryon number, and momentum conservation imply that constraints must be satisfied by the weight functions

$$\hat{W}_v(N=1, A, Z) = 1, \quad (11)$$

$$\begin{aligned} u_v^A(2, Q_0^2) + d_v^A(2, Q_0^2) + 2\bar{u}^A(2, Q_0^2) \\ + 2\bar{d}^A(2, Q_0^2) + g^A(2, Q_0^2) = 1. \end{aligned} \quad (12)$$

The best results are obtained using for valence distributions weight functions such as

$$\begin{aligned} W_v(y, A, Z) &= A [a_v \delta(1 - \epsilon_v - y) + (1 - a_v) \delta(1 - \epsilon_v - y)] \\ &+ n_v \left(\frac{y}{A} \right)^{\alpha_v} \left(1 - \frac{y}{A} \right)^{\beta_v} + n_s \left(\frac{y}{A} \right)^{\alpha_s} \left(1 - \frac{y}{A} \right)^{\beta_s}, \end{aligned} \quad (13)$$

where the first two terms may be interpreted as reduction in the parent nucleon longitudinal momentum fraction, and in spite of their simplicity accurately reproduce EMC and Fermi motion effects. Indeed, with just these three parameters the fit reproduces the large x_N data fairly well, however, it fails to account for antishadowing effects at intermediate x_N , where valence distributions still dominate.

In order to include antishadowing effects we add the third term in Eq. (13), which induces a small enhancement of the distributions with $n_v > 0$ and a mild x_N dependence given by the parameters α_v and β_v . Notice that the convolution integral dilutes the x_N dependence producing an effect similar to those predicted by parton recombination models [18]. It would be pointless to try to extract the nuclear modification to valence distributions in the low x_N region from the data, since this region is clearly dominated by sea and gluon densities, however, the first three terms in Eq. (13) violate charge conservation. In order to remedy this situation we include the fourth term, similar to the third but where charge conservation forces $n_s < 0$. In this case the weight function cannot be interpreted as a probability density but as the result of the mechanism that compensates rescaling and recombination effects. The parameters α_s and β_s are taken to be the parameters used for the sea quark densities, fixed by the low x_N behavior of the data, while both n_v and n_s are fixed by momentum and charge conservation, Eqs. (11) and (12).

For sea quarks and gluons, the argument is just the opposite: the fit to data is not sensitive to any nuclear modification at high or intermediate x_N , so the best choice for sea weight functions is found to be

$$W_s(y, A, Z) = A \delta(1 - y) + \frac{a_s}{N_s} \left(\frac{y}{A} \right)^{\alpha_s} \left(1 - \frac{y}{A} \right)^{\beta_s}, \quad (14)$$

where the first term gives the gluon distribution in free protons and the Eulerian function (specifically the parameter α_s) drives the low x_N shadowing (a_s is found to be negative). The three parameters a_s , α_s , and β_s are strongly constrained by the structure functions ratios at small x_N and the

Drell-Yan ratios. N_s is just the normalization of the Eulerian function $N_s = B(\alpha_s + 2, \beta_s + 1)$. Similarly, for gluons

$$W_g(y, A, Z) = A \delta(1-y) + \frac{a_g}{N_g} \left(\frac{y}{A}\right)^{\alpha_g} \left(1 - \frac{y}{A}\right)^{\beta_g}. \quad (15)$$

Here a_g is strongly constrained by the Q^2 -dependent F_2^{Sn}/F_2^C data, whereas the exponents are taken to be the same as for the sea distributions and $N_g = N_s$. No significant improvement is found assigning independent parameters for them. Since n_v and n_s are constrained by momentum conservation in Eqs. (11) and (12), there are 9 independent parameters $\epsilon_v, \epsilon_{v'}, a_v, \alpha_v, \beta_v, \alpha_s, \beta_s$, and a_g for each nucleus. Since no data are available on different isotopes of the same nucleus, in the following we drop the dependence on Z . The A dependence of all the parameters can be written

$$\epsilon_i = \gamma_i + \lambda_i A^{\delta_i}. \quad (16)$$

The full parametrization of both the A and x_N dependence of nuclear effects imply in principle quite a lot of parameters (27), however, the mild A dependence found in some of them allows us to reduce their number. For example, α_s, α_v , and a_v can be taken as constant in A losing just a few units in χ^2 but eliminating 6 parameters.

III. RESULTS

In the following section we present results from the LO and NLO fits to nuclear data using the convolution approach. The data analyzed include the most recent NMC and SLAC-E139 DIS structure functions ratios to deuterium and carbon, selecting those measurements corresponding to $Q > 1$ GeV, and also E772 Drell-Yan dilepton cross sections from proton nucleus collisions, as listed in Table I, rendering a total number of 420 data points.

The parameters were fixed minimizing the function χ^2 defined in the customarily way as

$$\chi^2 \equiv \sum_i \frac{(\sigma_i^{ex} - \sigma_i^{th})^2}{\Delta_i^2}, \quad (17)$$

where σ_i^{ex} stands the measured observable, σ_i^{th} the corresponding NLO (LO) estimate, Δ_i the statistical and systematic errors added in quadrature, and the sum runs over all the data points i included in the fit. No artificial weight has been given to any particular subset of data.

In order to compute the structure function and Drell-Yan cross section for deuterium, for which we neglect the nuclear corrections, and as a basis to construct the observables for the different nucleus, we use the parton distributions in the *free* proton as provided by the GRV98 analysis [16]. Consequently, we fix the initial scale to $Q_0^2 = 0.4$ GeV² (0.26 GeV²) and the QCD scale (for five flavors) $\lambda_{\text{QCD}}^{(5)} = 167$ MeV (132 MeV) to NLO (LO) accuracy. The total χ^2 obtained is 299.91 units for the NLO fit and 316.35 for the LO one.

TABLE I. Nuclear data included in the fit.

Measurement	Collaboration	Refs.	No. data
$F_2^{\text{He}}/F_2^{\text{D}}$	NMC	[9]	18
	SLAC-E139	[10]	18
$F_2^{\text{Be}}/F_2^{\text{D}}$	SLAC-E139	[10]	17
$F_2^{\text{C}}/F_2^{\text{D}}$	NMC	[9]	18
	SLAC-E139	[10]	7
$F_2^{\text{Al}}/F_2^{\text{D}}$	SLAC-E139	[10]	17
$F_2^{\text{Ca}}/F_2^{\text{D}}$	NMC	[9]	18
	SLAC-E139	[10]	7
$F_2^{\text{Fe}}/F_2^{\text{D}}$	SLAC-E139	[10]	23
$F_2^{\text{Ag}}/F_2^{\text{D}}$	SLAC-E139	[10]	7
$F_2^{\text{Au}}/F_2^{\text{D}}$	SLAC-E139	[10]	18
$F_2^{\text{Be}}/F_2^{\text{C}}$	NMC	[11]	15
$F_2^{\text{Al}}/F_2^{\text{C}}$	NMC	[11]	15
$F_2^{\text{Ca}}/F_2^{\text{C}}$	NMC	[11]	15
$F_2^{\text{Fe}}/F_2^{\text{C}}$	NMC	[11]	15
$F_2^{\text{Pb}}/F_2^{\text{C}}$	NMC	[11]	15
$F_2^{\text{Sn}}/F_2^{\text{C}}$	NMC	[12]	145
$\sigma_{\text{DY}}^{\text{C}}/\sigma_{\text{DY}}^{\text{D}}$	E772	[13]	9
$\sigma_{\text{DY}}^{\text{Ca}}/\sigma_{\text{DY}}^{\text{D}}$	E772	[13]	9
$\sigma_{\text{DY}}^{\text{Fe}}/\sigma_{\text{DY}}^{\text{D}}$	E772	[13]	9
$\sigma_{\text{DY}}^{\text{W}}/\sigma_{\text{DY}}^{\text{D}}$	E772	[13]	9
Total			420

The comparison between the data on the ratios of different nuclear structure functions to deuterium and those computed with NLO NPDF is shown in Fig. 1 (the LO prediction one is almost indistinguishable). The solid line corresponds to the result of the fit computed at the Q^2 value of each experimental point, whereas the extrapolation to small x_N has been

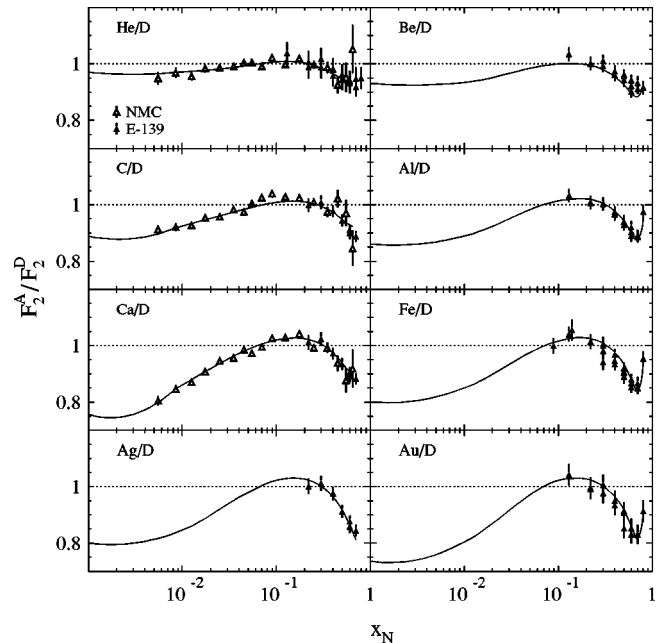


FIG. 1. F_2^A/F_2^D data. The lines interpolate the values obtained with the NLO NPDF set at the respective Q^2 , and extrapolate to low x_N at the Q^2 leftmost point.

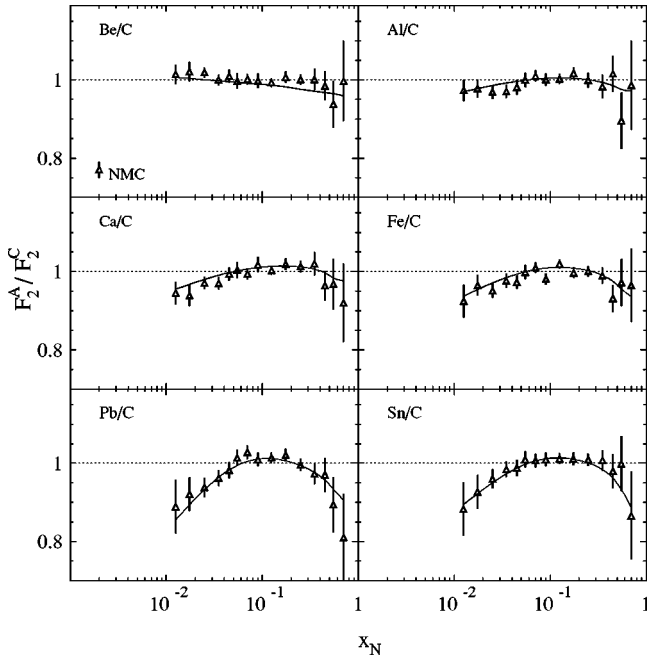


FIG. 2. The same as Fig. 1 but for F_2^A/F_2^C data.

performed using the corresponding Q^2 of the smallest- x_N point. For heavy nuclei, the low x_N is mainly constrained by DIS ratios to carbon, as shown in Fig. 2. The structure function ratios are useful to determine mainly the valence quark distributions, while Drell-Yan data, shown in Fig. 3 become crucial in order to fix sea quark distributions. The gluon distribution enters the structure function at NLO or through the scale dependence of the parton densities, making it very difficult to obtain information about it in DIS experiments. The Q^2 dependence of F_2^{Sn}/F_2^C , shown in Fig. 4, is the most sensitive available observable to the gluon distribution. Nevertheless, it is worth pointing out that there is still a large uncertainty on this density and data from observables where the gluon distribution enters at the lowest order, as in hadronic colliders, are needed to obtain a much better constraint.

The regular A dependence of the parameters, as observed in Fig. 5, helps us to interpolate through regions where the

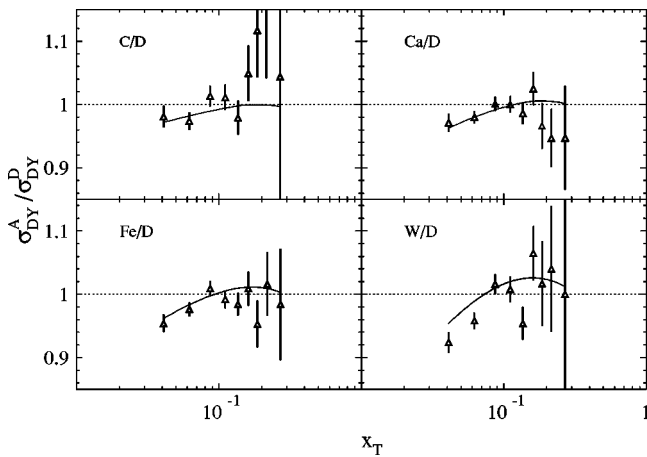


FIG. 3. Data on nuclear Drell-Yan cross sections rates to deuterium and those computed with NLO NPDF.

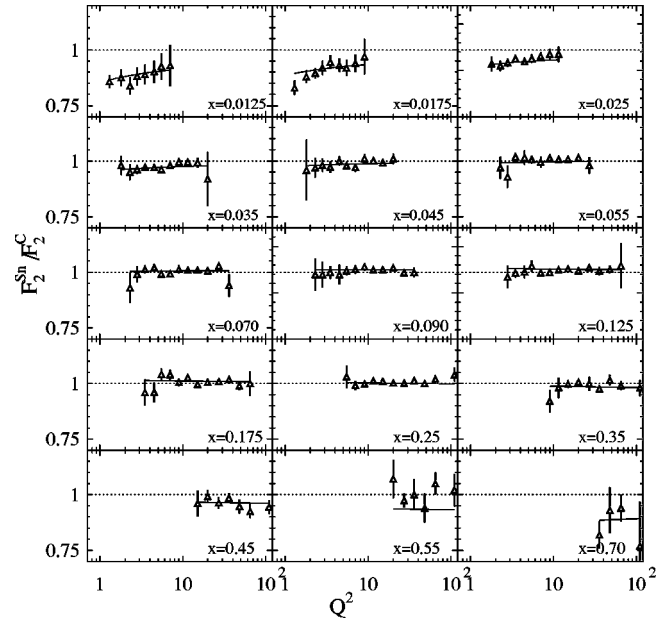


FIG. 4. Scale dependence of F_2^{Sn}/F_2^C data and the outcome of NLO NPDF.

data is scarce and also leads to reasonable extrapolations where there are none available. Noticeably, while some parameters show a clear dependence on the size of the nucleus, such as the shifts in the momentum fractions ϵ and ϵ' which drive nuclear effects at moderate and large x_N , those related to the shape of the nucleus effective densities at small x_N , such as α_v , α_s , and $\alpha_g = \alpha_s$ are not strongly dependent on A . The well known A dependence of shadowing effects at small x_N is driven by the normalization of these effective densities a_s and a_g , and also by the large x_N behavior of the densities fixed by the parameters β_v and β_s , which control

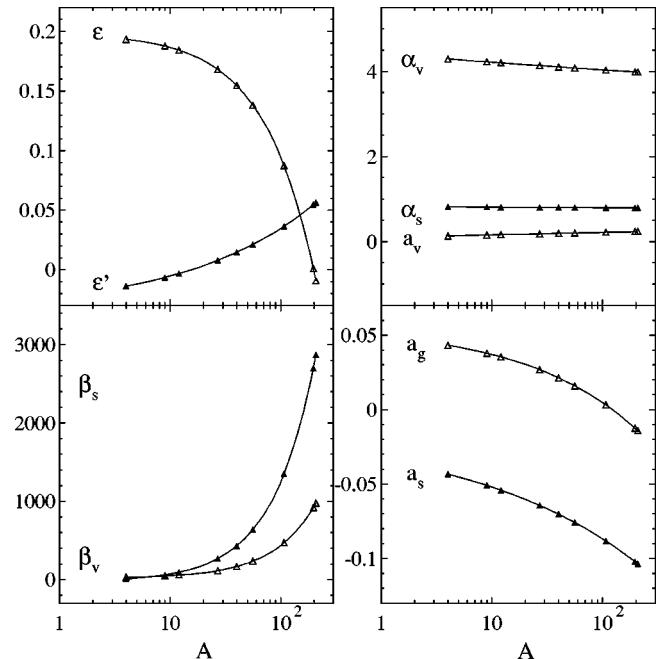


FIG. 5. A dependence of the parameters.

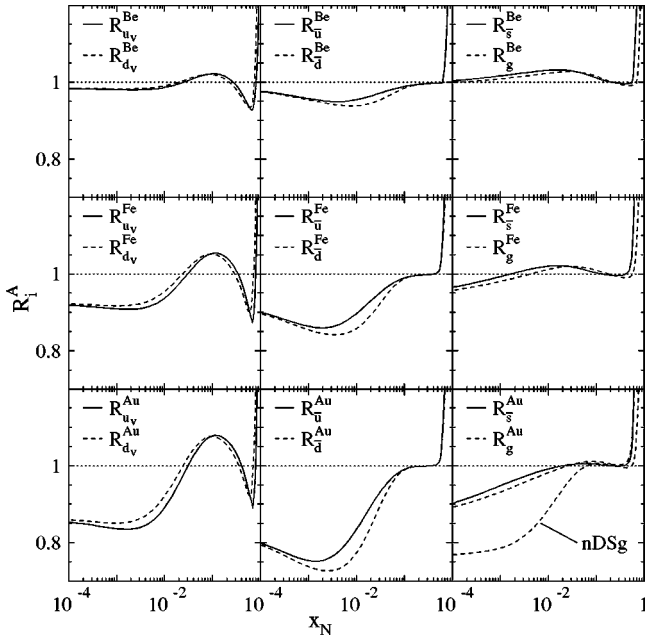


FIG. 6. The ratios for the densities are computed at 10 GeV^2 .

how much of the large x_N component of the PDF enters the convolution.

The resulting NPDFs are shown in Fig. 6, as ratios to free proton PDF, as defined in Eq. (2), for valence quarks, light sea and strange quarks, and gluons, at $Q^2=10 \text{ GeV}^2$. The numerical computation of these ratios once the NPDFs have been written and extracted within the convolution approach, is straightforward and allows a comparison with standard analyses, and other parton distribution functions. The ratios are also provided (in a FORTRAN code) as grids in x_N , Q^2 , and A for practical purposes and can be obtained upon request from the authors.

Similar results are found using nucleon parton densities other than GRV98. The similarity between modern parton densities guarantees that the nuclear ratios obtained with a given PDF set lead to reasonable NPDFs when combined with another. Therefore, the parton distribution in a nucleus A can be simply obtained by multiplying the nuclear ratios obtained in our analysis by any modern set of proton PDF. Of course, this is true provided the distributions come from analyses at the same order in QCD, as we will discuss in the next section.

It is worth mentioning that the agreement between nuclear parton distributions and data is remarkably better in the case of convolution-based parametrizations than the ones found with multiplicative parametrizations in previous (LO) analyses. Those analyses yield χ^2 values around 630 in the case of Ref. [6], and even larger values with the parametrization of Ref. [7], for the same data set used in the present analysis. A detailed comparison with the parametrization of Ref. [6] indicates that the χ^2 of that set is basically due to a large contribution from the Q^2 dependence of $F_2^{\text{Sn}}/F_2^{\text{C}}$ data. Therefore, one might expect significant differences between our LO gluon nuclear ratio and that of EKS98.

In Fig. 7 we show a comparison between the nuclear

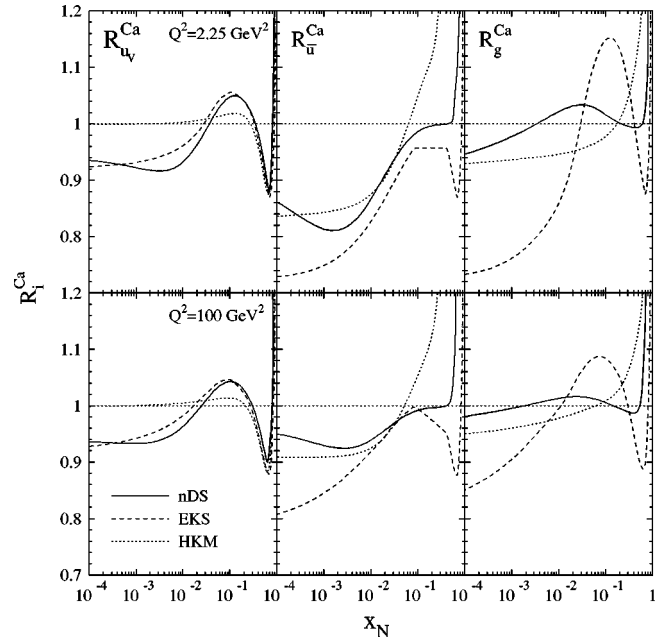


FIG. 7. Ratios coming from different NPDF sets.

ratios for LO u_{valence} , \bar{u} , and g proton (in calcium) distributions from NDS, EKS98, and HKM sets, at $Q^2=2.25 \text{ GeV}^2$ and 100 GeV^2 . The main differences with previous nuclear parametrizations are found in gluon densities, and to a lesser extent in sea quarks, when comparing with EKS98, and in valence and sea quarks in the case of HKM. Our gluon densities show comparatively less small x_N shadowing for heavy nuclei than EKS98, and very little antishadowing at intermediate x_N , which is considerable in their distributions. For nuclei lighter as C our gluons show only a tiny antishadowing effect.

In order to study the sensitivity of different observables on the amount of shadowing in the nuclear gluon distribution, we have performed an alternative extraction of NPDFs from the same data set but constraining the gluon density in heavy nuclei to show a stronger shadowing effect at small x_N . We provide the result in a set called NDSg, constrained to satisfy $R_g^{\text{Au}}=0.75$ at $x_N=0.001$ and $Q^2=5$. The χ^2 value of this analysis is around 550, considerably larger than the *unconstrained* fit, and should be considered only as a means to study variations on, mainly, the gluon nuclear distribution. An example for the gluon nuclear ratio in Au is shown in the last plot in Fig. 6.

Compared with HKM, our valence distributions show low x_N shadowing, whereas in HKM there is none. In our parametrization the ratios for sea and gluon densities approach unity as x_N grows, while with HKM distributions these ratios show a strong rise. The difference in the fits may be understood due to the fact that both the low x_N region in valence densities, and the large x_N behavior of the sea distributions have little impact on DIS observables, and is only picked up by Drell-Yan yields, not included in HKM analysis.

IV. NLO

Although there are no significant differences between the total χ^2 values obtained in LO and NLO fits, the corre-

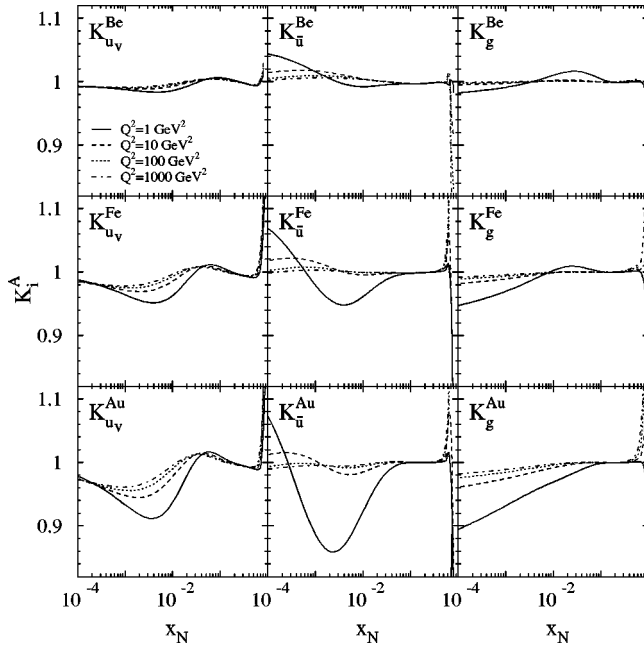


FIG. 8. Ratios between NLO and LO extractions of nuclear effects for different nuclei.

sponding NPDFs, and also the ratios of ordinary PDFs $R_i(x_N, Q^2, A)$, indeed differ, specially at low Q^2 . In some cases, the differences are as large as the nuclear effects themselves. In Fig. 8 the ratios between the NLO and LO extractions of $R(x_N, Q^2, A)$

$$K_i^A(x_N, A, Q^2) \equiv \frac{R_i^{\text{NLO}}(x_N, Q^2, A)}{R_i^{\text{LO}}(x_N, Q^2, A)} \quad (18)$$

are shown as a function of x_N for various Q^2 and different nuclei.

The main differences between $R_i^{\text{NLO}}(x_N, Q^2, A)$ and $R_i^{\text{LO}}(x_N, Q^2, A)$ are found in sea quark and gluon densities, most noticeably at low x_N and in heavy nuclei. These differences are correlated through the scale dependence with a similar behavior in the valence ratios at small x_N . As one would expect, the differences are more significant at small Q^2 and fade away as Q^2 increases.

The fact that LO analyses lead to fits comparable in accuracy to NLO analyses is due to the relatively moderated range in Q^2 spanned by the data, and the absence in the data set of nuclear observables strongly dependent on the gluon distributions. This, of course, does not imply that the differences in $R(x_N, Q^2, A)$ as obtained at LO and at NLO accuracy would be negligible, in fact, beyond LO the ratios are factorization scheme dependent. Nor does it imply that there would not be significant NLO corrections in other observables. This is particularly true for those that rely on the gluon or sea quark densities and stress the importance of having NLO extractions of NPDFs.

As an example of an observable which is sensitive to NLO corrections, in Fig. 9 we show the LO and NLO leading twist cross sections for the production of neutral pions in d -Au collisions as a function of the transverse momentum p_T

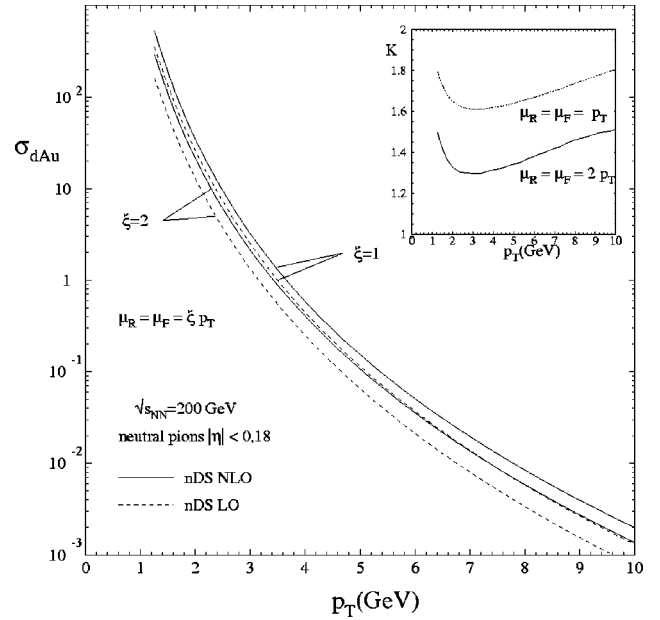


FIG. 9. LO and NLO neutral pion production cross sections for d -Au collisions.

of the final state particle. The plots correspond to nucleon center of mass energies $\sqrt{s_{NN}}$ of 200 GeV and a range in pseudorapidity of $|\eta| < 0.18$, computed using the code in Ref. [19] adapted for nuclear beams. Pion fragmentation functions were taken from Ref. [20]. The LO and NLO cross sections are computed at two different values for the factorization and renormalization scales $\mu_R = \mu_F = p_T$ and $\mu_R = \mu_F = 2p_T$. The differences between both predictions give an estimate of the theoretical uncertainty in the fixed order calculation. As can be observed, there is a considerable reduction in the scale dependence of the cross section when the NLO corrections are taken into account. This feature is found

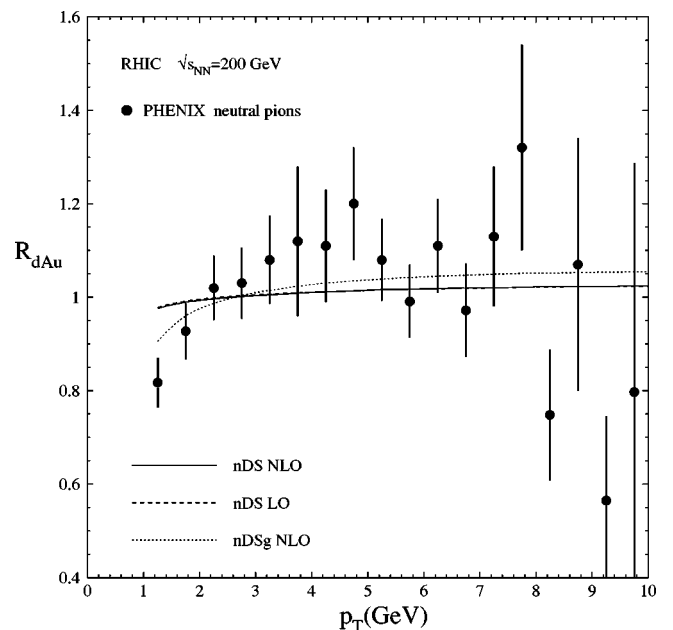


FIG. 10. Neutral pion production nuclear rates.

TABLE II. Parameters of the NLO and LO NPDP.

Parameter	NLO			LO		
	γ	λ	δ	γ	λ	δ
ϵ_v	0.1984	-0.0013	0.0814	0.2030	-0.0014	0.9510
ϵ'_v	0.0346	-0.0124	0.9421	0.0351	-0.0133	0.3657
a_v	0.7546	-0.6687	-0.0473	0.7251	-0.6647	-0.0583
α_v	2.1412	2.2690	-0.0390	2.1786	2.5720	-0.0439
β_v	-0.0474	0.3730	1.1301	19.925	2.2760	1.1463
a_s	-0.0135	-0.0202	0.2797	-0.0179	-0.0189	0.2664
α_s	0.7980	0.0814	-0.8647	1.0616	0.0572	-0.6277
β_s	-24.325	7.3191	1.1204	-24.107	7.3526	0.4284
a_g	0.0565	-0.0073	0.4244	0.0629	-0.0076	0.4285
χ^2/N_{DF}	299.91/393			316.35/393		

in almost any infrared-safe observable in hadronic collisions, indicating that LO calculations can only provide a qualitative description. The inset in Fig. 9 shows the K_{NLO} factor, defined as

$$K_{NLO} = \frac{\sigma_{dAu}^{NLO}}{\sigma_{dAu}^{LO}}, \quad (19)$$

i.e., the ratio between the NLO and LO cross section, computed at a given factorization and renormalization scales, and using the corresponding NPDPs and fragmentation functions. Notice that the K_{NLO} factor is not a physical quantity, actually it turns out to be strongly scale dependent, but provides an estimate of the size of the NLO corrections. In this case, it shows that the one-loop QCD corrections for pion production at RHIC are of the order of 50% or even larger, while the strong increase in the correction when the transverse momentum p_T is smaller than ~ 2 GeV indicates we approach the limit of the region of validity of PQCD calculations.

Finally, in Fig. 10 we show the estimates for the d -Au cross sections to neutral pions but normalized to proton-proton cross sections, against the data reported by Ref. [21], and not included in the present fit. With the exception of the lowest p_T data, which is on the borderline of the perturbative domain, the estimate agrees with the data well within the experimental uncertainties. Notice that even though the LO and NLO cross sections differ substantially, the discrepancies almost cancel in the ratios, to proton, highlighting the perturbative stability and the consistency between the LO and the NLO extractions of NPDPs. To quantify the effect of nuclear shadowing in the gluon distribution on hadron production at RHIC we have computed the same observable using the al-

ternative NLO set of NPDPs (set NDSg) with a larger shadowing in the gluon distribution at small x_N . Figure 10 shows a reduction in the d -Au cross section at small p_T for the set with larger gluon shadowing, however, it seems unlikely to obtain a much smaller value for the ratio R_{dAu} at $p_T \sim 2$ GeV with realistic NPDPs. Notice that the cross sections receive contributions typically from $x_N > 0.01$. Similar conclusions, with a slightly bigger reduction at small p_T , are reached if the same observable is computed for neutral pion production in the forward region ($\eta \sim 3$). Any experimental finding on a stronger reduction of R_{dAu} might certainly be considered as evidence of new phenomena, at least beyond PQCD. In Table II, we present the parameters of the LO and NLO NPDP.

V. CONCLUSIONS

We have performed for the first time a full NLO QCD global analysis of nuclear DIS and Drell-Yan data using a convolution approach to parametrize NPDP. We have found that this strategy not only leads to much more accurate NPDPs but considerably simplifies the numerical computation of QCD corrections at NLO. Although both LO and NLO NPDPs reproduce the available data with comparable precision, they show non-negligible differences which have to be taken into account when computing other observables.

ACKNOWLEDGMENTS

We warmly acknowledge W. Vogelsang for interesting discussions and suggestions. This work was partially supported by Conicet, ANPCyT, UBACyT and Fundaci3n Antorchas.

- [1] J.J. Aubert *et al.*, Phys. Lett. **123B**, 275 (1983).
 [2] M. Arneodo, Phys. Rep. **240**, 301 (1994).
 [3] S.S. Adler *et al.*, Phys. Rev. Lett. **91**, 072301 (2003); J. Adams *et al.*, *ibid.* **91**, 172302 (2003).
 [4] A. Accardi *et al.*, hep-ph/0308248.
 [5] E.H. Paschos and J.Y. Yu, Phys. Rev. D **65**, 033002 (2002).

- [6] K.J. Eskola, V.J. Kolhinen, and P.V. Ruuskanen, Nucl. Phys. **B535**, 351 (1998); K.J. Eskola, V.J. Kolhinen, and C.A. Salgado, Eur. Phys. J. C **9**, 61 (1999); Nucl. Phys. **B535**, 351 (1998).
 [7] M. Hirai, S. Kumano, and M. Miyama, Phys. Rev. D **64**, 034003 (2001).

- [8] C.A. García Canal *et al.*, Phys. Rev. Lett. **53**, 1430 (1984).
[9] P. Amaudruz *et al.*, Nucl. Phys. **B441**, 3 (1995); M. Arneodo *et al.*, *ibid.* **B441**, 12 (1995).
[10] J. Gomez *et al.*, Phys. Rev. D **49**, 4348 (1994).
[11] M. Arneodo *et al.*, Nucl. Phys. **B481**, 3 (1996).
[12] M. Arneodo *et al.*, Nucl. Phys. **B481**, 23 (1996).
[13] D.M. Alde *et al.*, Phys. Rev. Lett. **64**, 2479 (1990).
[14] D. de Florian *et al.*, Z. Phys. A **350**, 55 (1994).
[15] E.G. Floratos, D.A. Ross, and C.T. Sachrajda, Nucl. Phys. **B152**, 493 (1977); A. Gonzalez Arroyo, C. Lopez, and F.J. Yndurain, *ibid.* **B153**, 161 (1979); G. Curci, W. Furmanski, and R. Petronzio, *ibid.* **B175**, 257 (1980).
[16] M. Glück, E. Reya, and A. Vogt, Eur. Phys. J. C **5**, 461 (1998).
[17] Notice that this is not the case for the ratios R defined in x space as in Eq. (2).
[18] F. Close, J. Qiu, and R.G. Roberts, Phys. Rev. D **40**, 2820 (1989).
[19] D. de Florian, Phys. Rev. D **67**, 054004 (2003).
[20] S. Kretzer, Phys. Rev. D **62**, 054001 (2000).
[21] S.S. Adler *et al.*, Phys. Rev. Lett. **91**, 072303 (2003).